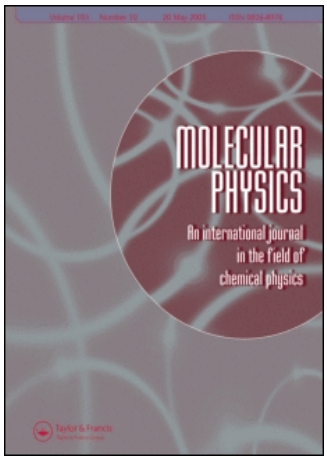

Molecular Physics
An International Journal in the Field of Chemical Physics
Publication details, including instructions for authors and subscription information:
http://www.informaworld.com/smpp/title~content=t713395160

A cooperative calculation and analysis of electric fields, induced dipole vectors and lattice energies for rotationally ordered ices IX, II and disordered Ih

Edwin S. Campbell [a]; Mihaly Mezei [ab]
[a] Department of Chemistry, New York University. New York, New York. U.S.A.
[b] Department of Chemistry, Hunter College. New York, New York

Online Publication Date: 01 November 1980
To cite this Article: Campbell, Edwin S. and Mezei, Mihaly , (1980) 'A cooperative calculation and analysis of electric fields, induced dipole vectors and lattice energies for rotationally ordered ices IX, II and disordered Ih', Molecular Physics, 41:4, 883 - 905
To link to this article: DOI: 10.1080/00268978000103231
URL: http://dx.doi.org/10.1080/00268978000103231

MOLECULAR PHYSICS, 1980, VOL. 41, NO. 4, 883–905

A cooperative calculation and analysis of electric fields, induced dipole vectors and lattice energies for rotationally ordered ices IX, II and disordered Ih

by EDWIN S. CAMPBELL and MIHALY MEZEI†
Department of Chemistry, New York University, New York, New York 10003, U.S.A.

(*Received* 20 *August* 1979 ; *revision received* 14 *June* 1980)

A non-additive model previously tested on 229 Hartree–Fock dimer energies and on trimer energies has been supplemented with different dispersion contributions and used to calculate the following properties of rotationally ordered ices IX and II and of disordeed Ih : (*a*) the different contributions to the lattice energy ; (*b*) the induced dipole vectors, electric fields and angle relations as a function of lattice site and of molecular orientation for Ih. The calculated results are discussed in terms of an interpretation of the preferred relative orientations of water molecules. The non-cooperative contribution for this model was found to be enhanced in a range from 50 to 100 per cent over that for trimer interactions.

1. INTRODUCTION

This paper reports calculations of the lattice energy, the induced and total dipole vectors and the local electric field in disordered and ordered forms of ice based on a model that has been proposed and tested [1, 2] on the water–water dimerization [3, 4] and the non-additive trimer [4, 5] and tetramer energies [4] based on wave-functions of near Hartree–Fock accuracy. It has been shown [1] that it reproduces 229 dimerization energies with an accuracy somewhat better than that of an alternative additive analytical model [3, 4] and that it provides a useful first approximation [1, 2] to the non-additive trimer and tetramer energies [4, 5]. This model for $U(n)$, the interaction energy of n molecules, consists of the following terms :

$$U(n) = U_p(n) + U_i(n) + U_d(n) + U_r(n). \tag{1}$$

U_p is the first order Coulomb interaction energy, $U_i(n)$ the non-additive contribution involving induced multipole moments, $U_d(n)$ the dispersion energy and $U_r(n)$ the repulsion energy. All calculations involve the following approximations to the general model (1). (i) $U_p(n)$ has been approximated with permanent multipole expansions for each molecule [6] (cf. also § 3.2). (ii) All terms in the derivatives of the fields have been neglected and in the calculation of the induced dipole vectors only linear terms in the field components, $\mathbf{E}_{perm} + \mathbf{E}_{ind}$, evaluated at the oxygens, have been included [7, 8].

† Present address : Department of Chemistry, Hunter College, 695 Park Avenue, New York, New York 10021.

(iii) The spherically symmetric function of [1] has been used for $U_r(n)$ and alternative spherical approximations for $U_d(n)$ (cf. § 3.2) have been tested. The algorithms developed and their tests have been given in other publications [1, 6, 9–13].

While the previous work was in progress, Jeziorski and van Hemert [14] reported a variation–perturbation calculation of the energy of dimerization of water. They noted that a calculation of the four contributions of (1) has the advantage of providing a simple physical model for the hydrogen bond.

2. Parameters for and relevant aspects of the molecular and crystal geometries

2.1. *Molecular geometry*

The intrinsic local frame has been chosen so that the molecule lies in the $(\mathbf{e}_1, \mathbf{e}_2)$ plane and $\mathbf{e}_1$ lies along the C_2-axis directed from the hydrogens to the oxygen. All calculations are based on the rigid nuclear geometry of Kistenmacher *et al.* [1 (*a*), 4], $d_{OH} = 0{\cdot}9572$ Å, $\measuredangle HOH = 104{\cdot}87°$, which is very close to the experimental geometry for the isolated monomer [15], $d_{OH} = 0{\cdot}95718$ Å, $\measuredangle HOH = 104{\cdot}523°$.

The extent of distortion in condensed phases is controversial. Studies of ices II and IX have shown increases varying from negligible to $\sim 0{\cdot}018$ Å and $1{\cdot}5°$ [16, 17] over the vapour O–D length, 0·9575 Å, and the DOD $\measuredangle$, 104·474° [15]. Conversely, increases by $\sim 0{\cdot}04$–$0{\cdot}05$ Å and $\sim 5°$ for ice Ih [18, 19] and by 0·02 Å for $D_2O(l)$ [20] have been reported. Still other arguments based on data of various types [16, 21] have led to our surmize that the O–D bond is stretched in condensed phases by perhaps $\sim 0{\cdot}01$ Å.

2.2. *Ice Ih*

The O sites of Ih belong to the space group, Schoenflies symbol D_{6h}^4 (International symbol, $P6_3/mmc$), one of the two suggestions of Barnes [22]. Let

$$\mathbf{a}_1', \mathbf{a}_2' : \text{2 unit cell vectors of hexagonal symmetry separated by an angle of } 120°\text{ ; } \mathbf{a}'_3 : \text{the unit cell vector } \perp \text{ to the } (\mathbf{a}'_1, \mathbf{a}'_2)\text{-plane.} \quad (2)$$

The unit cell has four distinct O positions whose fractional coordinates relative to the conventional origin are :

$$\left.\begin{array}{l} (a)\ (1/3, 2/3, 1/16)\,; \quad (b)\ (2/3, 1/3, -1/16)\,; \\ (c)\ (1/3, 2/3, 7/16)\,; \quad (d)\ (2/3, 1/3, 9/16). \end{array}\right\} \quad (3)$$

If all O–O distances were equal and all O–O–O angles had the ideal tetrahedral value of 109° 28′ 16·4″ = 109·471°, then

$$\|\mathbf{a}'_3\| / \|\mathbf{a}'_1\| = (8/3)^{1/2} \cong 1{\cdot}63299.$$

Experimental evidence supports a small deviation of uncertain magnitude from the ideal geometry [18, 19, 21–26]. The more consistent lower temperature data [24] give $\|\mathbf{a}'_3\| / \|\mathbf{a}'_1\|$ 1·6279 ; Av. Dev. $= \pm 0{\cdot}0006_8$ with no consistent trend in temperature. The differences in O–O distances have been either statistically insignificant [25 (*a*)] or marginally significant, 0·003 Å [19]. Conversely, the two distinct O–O–O angles appear to be different [25 (*a*)]

and are 8′ (5′) less (greater) than the ideal tetrahedral value, 109° 28′ 16″ [19]. Scherer and Snyder [26] suggested that their measurement of the intensity ratio for ν_3 and of the integrated intensities for H_2O and D_2O might be interpreted in terms of H-bonding more nearly linear when the O–O line parallels the c axis. Since the deviations are small and uncertain, the ideal geometry has been assumed. Then the distances become a function of the single O–O nearest neighbour distance, r_0. The latter was estimated in four different ways as described in Appendix 1.

Consider next the orientations of the hydrogens. Pauling [27] interpreted the difference between the spectroscopically calculated and calorimetrically measured entropy of ice [28] in terms of random orientations of the hydrogens subject to the following restrictions :

(i) the crystal contains only H_2O molecules ;
(ii) the H_2O are oriented to place one H approximately on each line between each pair of nearest neighbour O positions. (4)

This interpretation has been supported by such evidence as : (i) Nagle's [29] graph theoretical analysis of sets of orientations consistent with Pauling's rules gave $S(0\text{ K}) = 0{\cdot}8145 \pm 0{\cdot}0002$ eu compared with the experimental $S(0\text{ K}) = 0{\cdot}82 \pm 0{\cdot}05$ eu ; (ii) diffraction data as reviewed by Kamb [30] and confirmed at 77 K, which is below the temperature at which anomalies in the specific heat and elastic moduli had been reported ; (iii) dielectric constant studies [31] and by the failure to find any evidence for a ferroelectric transition which had been suggested [32]. Nevertheless, recently attention has been again called to the possibility of partial order parallel to the $\mathbf{a}'_3$ axis [33].

Since the occurrence of disorder implies that the energy difference between any two sets of orientations consistent with Pauling's rules (4) must be small compared to kT in any temperature range in which the energy barrier permits reorientation at an experimentally significant rate, it was desirable to determine the predictions of the model for different sets of orientations. Because of the conditional convergence of dipole–dipole lattice sums [34] it was important to use the technique employed in a previous study [35], which is analogous to the model used in simulation studies of liquids. Let : $z_{000} \equiv$ the set of four distinct positions given by (3) for a unit cell for O-positions ; $z_{ijk} \equiv$ a similar set given by i, j, k unit translations along the $\mathbf{a}'_1$, $\mathbf{a}'_2$, $\mathbf{a}'_3$ axes, respectively. Then all sets of orientations consistent with (4) were investigated for a lattice with a unit cell containing the 16 oxygen sites of

$$z_{000}z_{100}z_{010}z_{110}. \tag{5}$$

The effect of modelling the disordered structure by a crystal with such a small unit cell had been previously investigated by sampling the configurations for a unit cell with the 32 oxygen sites of $z_{000}z_{100}z_{010}z_{110}z_{001}z_{101}z_{011}z_{111}$. All the dipole–dipole energies for a sample of 840 sets of orientations lay between the extreme limits of those for the smaller cell [35]. The indexing of possible orientations which simplifies the following discussion is defined in Appendix 2.

2.3. *Ices III and IX*

Whereas dielectric dispersion measurements have provided clear evidence that at higher temperatures ice III is orientationally disordered [36], dielectric

constant measurements [37 (*a*)] indicated an ordering transition over a temperature range of pseudostability from $-65°$ to $-108°$C, apparently without change in the geometry of the oxygen sites, to a phase called ice IX. This view has been supported by the interpretation of I.R. spectra [38] and the entropy of phase transition [39, 40]. Since single crystal neutron diffraction data favour a structure in which 96 per cent of the D in $D_2O(s)$ are at sites for an ordered structure [17 (*a*)], the calculations reported in this article are based on perfect rotational order. Earlier single crystal X-ray diffraction [41] established a tetragonal unit cell $P_{4_12_12}$ for the O atom sites with

$$a = 6{\cdot}73 \pm 0{\cdot}01 \text{ Å}, \quad c = 6{\cdot}83 \pm 0{\cdot}01 \text{ Å} \quad (t = -175°\text{C}). \tag{6}$$

These values are for a state of pseudo-equilibrium in which the pressure has been released to 1 atm for the experimental measurements. They were assumed in the neutron diffraction studies and have been used in our calculations. However, $c/a = 1{\cdot}015 \pm 0{\cdot}003$ from (6) is not quite consistent with c/a from powder photographs [42] ($1{\cdot}044 \pm 0{\cdot}005$ at $-24°$C and 2·7 kbar for ice III and $1{\cdot}000 \pm 0{\cdot}003$ for ice IX at both 1 bar and 1 kbar).

The unit cell has the twelve following sites of two types : $O(I, j)$, $1 \leqslant j \leqslant 8$ at sites of no point symmetry ; $O(II, j)$, $9 \leqslant j \leqslant 12$ at sites on a twofold axis. The oxygen site coordinates used were derived by applying symmetry transformations to the neutron-diffraction data since they were accompanied by slightly smaller error estimates. Then the hydrogen coordinates for our monomer geometry (§ 2.1) were determined by adopting the neutron diffraction DOD angle bisectors and the DOD molecular planes. Appendix 3 gives the coordinates derived for all atoms in the unit cell and identifies the donor and acceptor nearest neighbours for each site.

2.4. *Ice II*

Evidence from I.R. spectra [38] and X-ray diffraction [43] that ice II has an ordered arrangement of hydrogens in the metastable state after pressure has been released to 1 atm was confirmed by single crystal neutron diffraction on $D_2O(s)$ at *ca.* $-110°$C [17 (*a*)]. The ΔS of transition to the rotationally disordered Ih [43 (*a*)], 0·5 R, and the absence of dielectric disperion throughout its range of stability [36 (*a*)] indicate that it is also ordered under pressure. The X-ray and neutron diffraction data were interpreted with the twinned rhombohedral $R\bar{3}$ structure. The X-ray data gave the unit cell parameters at $t = -150°$C [43 (*b*)] :

$$a = 7{\cdot}78 \pm 0{\cdot}01 \text{ Å}, \quad \alpha = 113{\cdot}1 \pm 0{\cdot}2°. \tag{7}$$

The unit cell contains 12 molecules of two types : $O(I, j)$, $1 \leqslant j \leqslant 6$; $O(II, j)$, $7 \leqslant j \leqslant 12$. Each type forms six-membered puckered rings. For these calculations the orientations of the monomers (§ 2.1) were determined by assigning them the experimental DOD angle bisectors and the DOD molecular planes. The coordinates of all sites in the unit cell and the identification of donor and acceptor nearest neighbours for each site are given in Appendix 4.

2.5. *Elements of the polarizability tensor*

Because of the agreement between the trace for the equilibrium positions $\bar{\alpha}_e = 9{\cdot}74$ au and $\bar{\alpha}_{expt} = 9{\cdot}82$, we adopted the values [44] used in the previous

study [1], despite the evidence [45] that the uncoupled Hartree–Fock technique leads to substantial errors. The errors for water are shown by comparison with coupled electron pair values [46] for the static tensor, for which the anisotropies have been estimated to be correct to 5–15 per cent, and which have been confirmed to better than these limits by Rayleigh depolarization data [47].

Source	α_e^{11}	α_0^{11}	α_e^{22}	α_0^{22}	α_e^{33}	α_0^{33}	$\bar{\alpha}_e$	$\bar{\alpha}_0$†
WM [46]	9·64	9·79	9·81	10·14	9·59	9·66	9·68	9·86
LM [44]	9·80		11·14		8·27		9·74	

(8)

3. Results and discussion

3.1. *Permanent multipole and induced dipole energies for ice Ih; energetic and symmetry interpretation of rotational disorder*

The overwhelming experimental evidence summarized above for the existence of rotational disorder in ice Ih and the successful interpretation of the entropy discrepancy by Pauling's model with equal statistical weights for all orientations consistent with (4) posed two problems for this study. First, as Rahman and Stillinger [48] observed, the evidence that the energy bias has minor effects on the proton distribution deserves a theoretical check, particularly since experimentalists have at times justifiably qualified the interpretations of their evidence for disorder by inclusion of a phrase such as '. . . no very significant change in proton ordering occurs . . .' [19 (*a*)]. The second problem was to determine the aspects of the water molecule responsible for this disorder.

The previous inference [35] of possible energy differences between configurations was limited by: (i) the use of point charge models (even though tested by a wide range of models); (ii) the consideration of only the first order electrostatic energy; (iii) the truncation of the corresponding permanent multipole representations using a single centre for each molecule at order 8, which left undesirably large error bounds [6]; (iv) the restricted number of different configurations considered. Since the range of energy differences seemed high (*ca.* 0·1 to 0·66 kcal mol^{-1}‡, cf. pp. 2704–5 and table XI [35]), this study was undertaken to eliminate or at least sharply reduce each limitation.

Since the energies of transition between the rotationally disordered Ih and the ordered form II have been estimated as only $\sim 0{\cdot}019$ kcal mol^{-1} [49 (*b*)] and between Ih and III (which at lower temperatures transforms to the ordered form IX) as of the order of 0·1 to 0·2 kcal mol^{-1}, compared with a lattice energy of 14 kcal mol^{-1} for ice Ih [50], it follows that a study of energy as a function of orientation for any assumed model should be carried to a consistency as near this order of magnitude as possible. Since the previous studies had shown that low order multipole approximations, which represent the symmetry of the molecule poorly, were completely inadequate for this purpose (e.g. the dipole–dipole and fourth order approximations gave as little as 24 and 83 per cent of the total permanent multipole lattice energies, respectively [35]), the present calculations included all orders $\leqslant 14$ to increase the accuracy of the

† The values are for the axis system assumed in § 2.1, the subscript 'o' refers to vibrationally averaged values. Multiplication of the entries by $1{\cdot}648\,776 \times 10^{-41}$ yields α in the units of C m/V m^{-1} = C^2 m^2/J.

‡ 1 kcal = 4·184 kJ.

representation of the molecular symmetry. The following evidence supports the conclusion that there is a small but definite difference between the permanent multipole contribution to the lattice energies of different hypothetical ordered configurations. The permanent multipole energy was computed for each of the 856 configurations consistent with the 16 molecule unit cell of (5)†. After division of all configurations into those 55 classes whose members all had identical energies for all permanent multipole interactions of order $\leqslant 5$ for any arbitrarily assumed charge distribution consistent with the symmetry of the water molecule [35], the members of each class had the same permanent multipole energy of order $\leqslant 14$ for this wave function. A heuristic estimate of the uncertainty due to the truncation of the multipole expansion is given by the greatest |(multipole energy for orders $\leqslant 14$)–(multipole energy for orders $\leqslant 13$)| which was found for any of the 55 classes. With $r_0 = 2{\cdot}72$ Å, this was 0·026 kcal mol^{-1}. Since the greatest absolute difference between the permanent multipole energies for orders $\leqslant 14$ between any pair of the 55 classes was 0·145 kcal mol^{-1}, this particular wave function predicts different permanent multipole contributions to the lattice energy for different hypothetical orientations. The entire set allows the comparison of alternative polar and non-polar structures (cf. Appendix 5 for other energetic consequences of a polar structure). The configurations, which like real Ih are non-polar, fall into 10 energy classes (cf. Appendix 2). At $r_0 = 2{\cdot}741$ Å, the greatest absolute difference in permanent multipole energies was 0·094 (0·135) kcal mol^{-1} or 0·47 (0·67 per cent) of the total permanent multipole contribution for the 10 (55) energy classes. Since the calculated dipole moment $\simeq 1{\cdot}2$ (experimental) and since the spread in dipole–dipole energies makes the greatest contribution, the energy difference may be ~ 30 per cent too large.

Next consider the contribution from the dipole which is induced at each site by the permanent multipoles and, cooperatively, by the induced dipoles at all other sites. Arguments at the end of this section, which support the inference that membership of a configuration in one of the above 55 energy classes is a consequence of certain symmetries of the water molecule and of the ice Ih lattice and does not depend on the character of the equations for the first order coulomb energy they define, are further substantiated by the fact that the same 55 classes were found to be valid for the induced dipole contribution as well. Induced calculations for different r_0 were executed for only one representative configuration from each energy class, defined for the set of 10 in Appendix 2. For $r_0 = 2{\cdot}741$ Å the maximum minus the minimum energies were 0·55 (1·07) kcal mol^{-1} for the 10 (55) classes. The arguments given below support the inference that the inclusion of higher order induced multipoles would lower this spread, just as the inclusion of higher order permanent multipoles lowered the spread of 0·60 (2·32) kcal mol^{-1} for dipole–dipole energies to 0·094 (0·135) for the 10 (55) energy classes.

The argument rests in part on the answer to the second problem posed at the beginning of this section. The evidence (*a–d*) below supports the conclusion that the three following aspects of the symmetry of water molecules lead to approximately tetrahedral coordination in condensed phases and to energy differences between possible orientations which are a small fraction of

† The number of configurations reported in a previous study [35] was reduced from 2970 to 856 by elimination of symmetry duplications.

the total lattice energy and, therefore, provide a qualitative basis for the existence of rotational disorder in the ice Ih structure: (i) the molecule has two positive and one negative centre in a molecular symmetry plane; (ii) the bond angle is approximately tetrahedral; (iii) the charge distribution is sufficiently assymmetric that the gain from optimizing the relative orientations more than balances the loss from the decrease in density compared to the close packed structure assumed by the related H_2S molecule [51]. (*a*) Neither of these structural features can be due to any tetrahedral symmetry of the monomer charge density. Although such a symmetry has often been inferred from the idea of lone pairs, Hankins' wave function of near Hartree–Fock accuracy did not show the expected approximately tetrahedral symmetry [52], and our calculations on the wave function of [53] showed that the maximum electron density in the lone pair plane did not occur at tetrahedral angles $\pm 54{\cdot}74°$ but in the molecular plane. (*b*) Conversely, a wide range of models with triangular or tetrahedral symmetry [35] yield energy differences which are a small fraction of the lattice energy†. Whereas the cylindrical symmetry of the dipole vector gives dipolar lattice energies which vary by a factor of about 2·6 for different configurations of ice Ih, when the symmetry of the models is more accurately reproduced by single centre multipole expansions of the eighth order about the O nucleus, the lattice energy differences are reduced to 5 per cent or less. (*c*) The following arguments suggest that the analytical fit [3, 4] using centrosymmetric point sources in the molecular plane at points at and near the corners of a triangle would also lead to differences which would be small compared to the lattice energy and of the same relative magnitude as we have found: (i) both the strictly additive [3, 4] and the present non-additive potentials reproduce the same HF dimer data [1]; (ii) the additive component $U_p + U_r$ of the latter leads to a relative energy difference between the ten energy classes of only 2·8 per cent at $r_0 = 2{\cdot}741$ Å. Their strictly additive [3, 4] should yield a similar result. (iii) Since a Monte Carlo calculation [54] using the analytical fit [3, 4] and a perturbation estimate for the dispersion contribution gave a reasonable representation of the O–O pair distribution function in $H_2O(l)$, it follows that the triangular symmetry when the molecular plane is a symmetry plane, the bond angle is approximately tetrahedral and the angular dependence is sufficiently strong suffices to yield the preferred approximately four coordinate structure even in the fluid phase. Conversely, the cylindrical symmetry of permanent dipoles should lead to a chain structure such as is observed in HCN(*s*) [55] and is distorted by other contributions to give staggered chains in HF(*s*) [56].

Finally, return to the problem of the much greater variation in the energy involving induced dipoles compared to the variation in the energy contributed by permanent dipoles alone. It follows from the above discussion of the symmetry of the water molecule and of the occurrence of rotational disorder in ice Ih that this range should be much smaller when the molecular symmetry is more satisfactorily represented by the inclusion of higher order induced multipoles just as the range for the permanent multipole energies is much smaller when the molecular symmetry is more adequately represented by the

† This has been established in unpublished calculations for a wide range of plausible parameters for the point charge models of [35] which reproduce the experimental dipole vector.

inclusion of higher order permanent multipoles than the range when the molecular symmetry is replaced by the qualitatively different symmetry of the permanent dipole approximation. This inference is also supported by the observation that the field defined by permanent multipoles and cooperatively by induced dipoles does not always give a vanishing net unit cell induced dipole even when the net permanent dipole vanishes. Thus, the net induced dipole vector for a unit cell of 16 molecules varies from 0 to 0·026 au for those ten orientations in which the net permanent dipole vector vanishes. This should be compared to an induced dipole vector of *ca.* 0·5 au per molecule.

3.2. *Lattice energies*

The calculations of the lattice energy, $U(\infty)$, by (1) correspond to the energy difference,

$$U(\infty) = \Delta U = U(g) - U(s) + (U_{\text{vibration}}(s) - U_{\text{vibration}}(g)).$$

Whalley's [50] careful estimate of ΔU for ice Ih gives a vibrational correction of 2·76 kcal mol^{-1} which, when added to the experimental heat of sublimation at 0 K, 11·315 kcal mol^{-1}, yields 14·08 kcal mol^{-1}. Unfortunately, no similar estimate was found either for ice II or ice IX. The size of the vibrational correction, which includes an intermolecular zero point energy correction of 3·95 kcal mol^{-1} which would be expected to be different for different lattices, precludes a direct comparison with experimental data for II and IX. The calculated results are shown in table 1 for the three different dispersion energy corrections defined in the legend.

Since the total lattice energies have been computed using a model that reproduces the 229 Hartree–Fock energies of dimerization of [3, 4], the calculated values are to be viewed as a test of supplementing Hartree–Fock pair energies with a dispersion and a particular non-additive contribution. Since the wave function used in the dimer calculations gives an equilibrium dimerization energy of 4·37 kcal mol^{-1} compared with a value of 3·67 kcal mol^{-1} of pairs from a wave function including *f*-type harmonics on O and *d*-type on the Hs, the calculated lattice energies should be expected to be too large. Even without taking into consideration the neglect of the angular dependence of the dispersion contribution, the agreement for ice Ih is at least as good as can be expected for both the dispersion models *a* and *b*. Whereas our result that ΔU for ice IX is somewhat less than for ice Ih is plausible, it seems unlikely that the zero point vibration correction for ice II should be enough larger than the 3·95 kcal mol^{-1} for ice Ih to account for the relative values for ice Ih and ice II. Since the sum of the permanent multipole and induced dipole contributions are in the expected order inferred from the compromise in preferred relative orientations caused by pressure ($|U_p + U_i|_{\text{Ih}} > |U_p + U_i|_{\text{IX}} > |U_p + U_i|_{\text{II}}$), and since the increased near neighbour distances in the more dense forms yields an angularly averaged dispersion contribution in the order Ih > II $\simeq$ IX, the discrepancy should probably be assigned to the anomalously low repulsive contribution for ice II. It seems to us that this may not be due to any inadequacy of the particular HF dimer potential, but the particularly simple form of U_r previously chosen to test the model [1], since even the use of three rather than two terms in U_r yielded a decrease in the standard deviation of the fit to the

Table 1. Lattice energy contributions for ice forms in kcal mol^{-1}.

Ice form	U_p	U_i	U_p+U_i	U_d (a)	(b)	(c)	U_r	Total (a)	(b)	(c)
Ih	−20·20	−7·02	−27·22	−3.78	−4·11	−6·57	+15·87	−15·12	−15·46	−17·91
II	−17·45	−7·74	−25·19	−3·34	−3·92	−7·34	+12·59	−15·94	−16·52	−19·94
IX	−18·29	−7·21	−25·50	−3·21	−3·92	−7·11	+13·75	−14·96	−15·67	−18·86

(i) U_p, U_i, U_d and U_r are defined by (1). (ii) The dispersion energies were calculated for the models of: (*a*) [57] (see [58] for comparison); (*b*) Kolos from [54]; (*c*) data [14] for a single orientation fit to the least squares equation for r in bohr, $U_d(\text{kcal mol}^{-1}) = -3{\cdot}8117 \times 10^3/r^6 - 2{\cdot}1810 \times 10^6/r^8 + 2{\cdot}0715 \times 10^7/r^{10}$. (iii) The value for Ih is the average of the 10 orientations with a vanishing net permanent dipole with $r_0 = 2{\cdot}741$ Å.

Hartree–Fock data from 0·0019 to 0·0012 and in the standard relative deviation from 0·19 to 0·16. A variation of this order could account for the difference.

Consider next the relative contributions to the lattice energy. The ratio [(interaction energy involving induced dipoles)/(interaction energy involving only permanent multipoles)] is (0·39, 0·44) for ices (IX, II) and varies over the range (0·336, 0·364) in the set of 10 classes for which the net permanent dipole vector vanishes. These ratios compare with the value 0·31 which Coulson and Eisenberg [59] obtained by a certain average over relative orientations consistent with Pauling's rules for ice Ih (cf. (4)). Since they used a permanent dipole moment of only 1·78 D and very different quadrupole and octupole moments, the similarity of their and our values for ice Ih suggests that the effects of differences in multipole moments and even of truncation at the octupole level are largely cancelled in the ratio.

The energetic importance of cooperativity for the ices was determined by calculating the contribution involving induced dipoles non-cooperatively, $U_i^{\text{non-coop}} \equiv$ the contribution using the dipole vectors which would be induced at each site by the **E** defined by only the permanent multipoles ignoring the cooperative contribution from the induced dipole vectors at other sites. This reduced $|U_i|$ by (2.12, 2.48) kcal mol^{-1} for ices (IX, II) and by amounts over the range (1·71, 2·19) kcal mol^{-1} for the 10 classes of ice Ih. These give the ratios $|(U_i - U_i^{\text{non-coop}})/U_i|$ of (0·32, 0·29) and (0·25, 0·30) and of $R \equiv |(U_i - U_i^{\text{non-coop}})/(U_p + U_i + U_r)|$ of (0·18, 0·20) and (0·15, 0·19), respectively. Thus the cooperative interaction through the lattice has enhanced R from $\bar{R} = 0{\cdot}10$ averaged over the frequency of trimer occurrence [5] in Ih.

Two points should be considered in the interpretation of these calculations. The first is the validity of the use of a multipole representation of the first order Coulomb energy. This is dependent upon the particular molecules since some tests [60, 61] have given useful approximations even at distances in condensed phases, whereas others [62, 63] yielded good (including HF) to useless results at van der Waals radii. After we had completed almost all calculations, Mulder and van Hemert [64] kindly provided us with a pre-publication comparison of the multipole approximation with the unexpanded first order Coulomb energy for one of the relative H_2O–H_2O orientations used by [14] and their H_2O wave function.

We repeated the multipole calculations using our split mode [6] including terms of order $\leqslant 14$. Their and our multipole expansions agreed within 6 per cent at 4 au and 0·6 per cent at ice distances. They found a difference of the order of 25 per cent at the nearest neighbour distances of ice Ih. The following arguments (*a*) and (*b*) lead us to believe that the difference must be much smaller. (*a* i) The preceding discussion has shown that an acceptable model for water should satisfy the following criterion : in the case of ice Ih, the values of lattice energy sums for different sets of water molecule orientations which are consistent with Pauling's rules (4) should differ by at most a small fraction of the lattice energy. This has been established for both permanent multipole sums which are only asymptotically convergent (e.g. the present work) and sums which are truly convergent (e.g. a wide range of point charge models for which the charges for different lattice sites are contained in disjoint spheres [35]). (*a* ii) Let the permanent multipole lattice sum for any set of orientations, O, for ice Ih be written as the sum of a nearest neighbour

contribution, O_N, and a sum of contributions from all more distant sites, O_d. Let O and O' be two different sets of orientations consistent with Pauling's rules (4). For many pairs O and O', $|O_N - O'_N| \gg |(O_N + O_d) - (O'_N + O'_d)|$. (*a* iii) The calculations of van Hemert and Mulder lead to the reasonable conclusion that the only significant discrepancy between the unexpanded evaluation of the first order Coulomb integral and the multipole expansion can occur in the lattice only for near neighbour sites. (*a* iv) If the difference between the unexpanded and expanded values at the nearest neighbour distance were ~ 25 per cent, the lattice sums for the first order Coulomb energy could satisfy the criterion of (*a* i) only if a positive difference for one nearest neighbour orientation were very nearly cancelled by a negative difference for another. This seems to us highly unlikely. (*b* i) Let us use the sequence of differences between permanent multipole sums of successive orders as a basis for an estimate of their asymptotic convergence. Let the relative error in the truncated asymptotically convergent series $\equiv$ |(error)/(permanent multipole sum)|. When the contributions of all orders $\leqslant 14$ were included, our expansions gave the following relative errors: a three centre expansion [6], $< 3 \times 10^{-5}$; a single centre expansion, $< 3 \times 10^{-3}$. The conservatism of our estimates is shown by the fact that our expansions had a relative difference of $8{\cdot}4 \times 10^{-4}$. (*b* ii) Our results on hundreds of pair interactions have shown that a large relative error for either type of expansion has always been reflected in a disagreement between their values. Whereas we would not be surprised by a substantial error in the permanent multipole sum for the first order Coulomb energy if the successive partial sums varied by a few per cent, we believe that a 25 per cent error in the multipole value for the nearest neighbour interaction in ice is unlikely when the relative error of the asymptotically convergent three centre expansion $< 3 \times 10^{-5}$.

The second point is the limitation of the non-additive contribution to terms involving induced dipoles. Recent results provide a further test of one of the limitations in this approximation. Calculations of the triple dipole interaction, the leading non-additive component of the dispersion contribution [65] indicate that it is about an order of magnitude smaller than the non-additive induced contribution for the very polar water molecule. Although the authors emphasize that they have calculated an approximation valid for long-range interactions, and although test calculations on three H atoms showed that in this case the approximation gives a useful representation of the non-additivity only at distances significantly greater than the van der Waals minimum for non-bonded interactions [66], it seems unlikely that for the closed shell water molecule, the errors in using the expanded form will be enough greater to alter the qualitative comparison. Thus, the induced contribution to non-additivity should be the more important one.

3.3. *Compression in condensed phases*

The minimum in the H_2O–H_2O dimer potential energy surface occurs at $d_{o-o} = 3{\cdot}00$ Å for the near Hartree–Fock wave function of [4] and at 2·924 Å for the extended CI wave function of [67]. These values compare with most probable nearest-neighbour distances in $H_2O(l)$ varying from 2·82 Å at 4°C

to 2·94 Å at 200°C [68]†. In ice Ih the nearest neighbour distance at 0°C is given as 2·76 to 2·77 Å [25 (*a*)] and extrapolation of the data of [23] gives 2·762 Å‡.

Consider first the compressive effect of the non-additive contribution [5]. Although the compressive effect of any contribution clearly depends upon how it varies with distance, the relative contribution of various factors to the equilibrium lattice energy should provide an approximate ordering of the significance of their contributions to the compression. For ice Ih, the discussion of lattice energies gives values of 15–19 per cent for the cooperative contribution. Another important compressive contribution in condensed phases is a minimization of the lattice energy by decreasing distances for attractive interactions with sites outside the nearest neighbour shell with the sacrifice of part of the nearest neighbour contribution as the distance decreases. The importance of longer range interactions is shown by the ratio $R_N \equiv \{U(\text{nearest neighbours})/U(\text{lattice})\}$. For ice Ih, R_N for the lead spherically averaged dispersion contribution is 0·78. The effect of the slower decrease with distance of the permanent multipole contribution is shown by an even smaller ratio. For one configuration of ice Ih and one charge model for H_2O, $R_N = 0{\cdot}63$ for all multipole interactions of order $\leqslant 4$ [35 (*d*)].

3.4. *Electric field vectors at the oxygen sites*

The values of the electric field vectors, $\mathbf{E}$, are of particular interest because of the frequent discussion of the local field. Whereas the field components with respect to a crystal based frame will exhibit no apparent pattern, their essential simplicity and symmetry should be clear in a local frame fixed with respect to the molecule at each site. Consider such orthogonal frames with centres at the oxygen sites and basis vectors :

$$\left.\begin{aligned} \mathbf{e}_1 &= -(\mathbf{OH}_\alpha + \mathbf{OH}_\beta)/\|\mathbf{OH}_\alpha + \mathbf{OH}_\beta\|, \\ \mathbf{e}_2 &= \mathbf{H}_\alpha\mathbf{H}_\beta/\|\mathbf{H}_\alpha\mathbf{H}_\beta\|, \\ \mathbf{e}_3 &= \mathbf{e}_1 \times \mathbf{e}_2. \end{aligned}\right\} \tag{9}$$

The major component of the electric field at a given site defined by the permanent multipoles of all other lattice sites lies along the HOH angle bisector and the variation in the field with configuration in ice Ih and with the site for ices Ih, IX and II are shown by table 2.

3.5. *Dipole vectors in ice*

It follows from § 3.4 that the same local systems (9) should be used for the discussion of the induced dipole vectors. The results are shown in table 3. Since the induced vectors were obtained from a cooperative calculation which includes the field contributions from induced dipole vectors at other sites, the variations with site, configuration of Ih and ice form, are in part due to the neglect of contributions from the derivatives of the field [7, 8].

† These diffraction curves have been confirmed by Hajdu, Lengyel and Palinkas [69]. However, the small scale graphs in their article and a later article by Narten [70] cannot be used to check the exact values reported for the first maximum in the earlier article.

‡ Their data for the *c*-axis length which are more consistent than their data for the a-axis length have been used and a perfect tetrahedral geometry has been assumed.

Table 2. $\mathbf{E}^{\mathrm{perm}}$ in ices Ih, IX, II in the local frame (9) (i).

Ice Ih configuration number (iii)	$\|\mathbf{E}^{\mathrm{perm}}\| \times 10^2$ Min (ii)	Max (ii)	$\{(E_2^{\mathrm{perm}})^2+(E_3^{\mathrm{perm}})^2\}^{1/2}/\|\mathbf{E}^{\mathrm{perm}}\|$ Max (ii)	Min (ii)
412	4·09	4·10	$9{\cdot}66\times10^{-3}$	$1{\cdot}22\times10^{-3}$
329	4·04	4·14	$1{\cdot}24\times10^{-2}$	$1{\cdot}95\times10^{-2}$
352	4·04	4·13	$1{\cdot}80\times10^{-2}$	$1{\cdot}21\times10^{-2}$
363	4·04	4·11	$8{\cdot}99\times10^{-3}$	$9{\cdot}73\times10^{-3}$
108	4·07	4·10	$4{\cdot}66\times10^{-3}$	$1{\cdot}48\times10^{-2}$
326	4·04	4·13	$2{\cdot}57\times10^{-3}$	$9{\cdot}76\times10^{-3}$
22	4·00	4·14	$9{\cdot}44\times10^{-3}$	$9{\cdot}17\times10^{-3}$
17	4·00	4·13	$1{\cdot}10\times10^{-2}$	$5{\cdot}45\times10^{-3}$
338	4·00	4·16	$9{\cdot}04\times10^{-3}$	$2{\cdot}88\times10^{-3}$
57	4·01	4·11	$1{\cdot}78\times10^{-3}$	$1{\cdot}03\times10^{-3}$
Ice II (iv)	3·94 (I)	4·33 (II)	$5{\cdot}28\times10^{-2}$	$1{\cdot}03\times10^{-1}$
Ice IX (iv)	4·03 (I)	4·15 (II)	0	$1{\cdot}56\times10^{-1}$

(i) $\mathbf{E}^{\mathrm{perm}}$ was calculated for each oxygen site as the electric field defined by the permanent multipoles of all other lattice sites. Single centre expansions of order 13 were used at each oxygen site. The values are in units of (electron charge)/(bohr)^2. Multiplication by $5{\cdot}142\,250\times10^{11}$ gives $\mathbf{E}$ in V m^{-1}. (ii) $\|\mathbf{E}^{\mathrm{perm}}\|_{\mathrm{Max}}$ is the greatest, $\|\mathbf{E}^{\mathrm{perm}}\|_{\mathrm{Min}}$ is the least $\|\mathbf{E}^{\mathrm{perm}}\|$ as a function of site in the unit cell. (iii) The ten configurations for ice Ih were chosen as representatives from each of the ten classes with a zero net dipole vector. They are defined in table 5 of Appendix 2. (iv) (I) and (II) refer to the lattice site types(cf. §§ 2.3, 2.4). (v) The Ih values are for $r_0=2.741$ Å.

Table 3. Dipole vectors (*a*).

Ice Ih (*f*) number (*d*)	$\|\mu_{\mathrm{ind}}\|$ Min (*c*)	Max	$\|\mu_{\mathrm{tot}}\|$ Min (*c*)	Max	θ (*b*) Min (*c*)	Max	$\|\mu_{\mathrm{ind}}\|/\|\mu_{\mathrm{tot}}\|$ Min (*c*)	Max
412	0·572	0·572	1·436	1·437	0·357	0·624	0·398	0·398
329	0·534	0·573	1·398	1·437	0·053	1·557	0·382	0·399
352	0·546	0·559	1·410	1·424	0·482	0·810	0·387	0·393
363	0·549	0·556	1·413	1·421	1·074	1·161	0·388	0·392
108	0·550	0·555	1·414	1·420	0·821	1·419	0·389	0·391
326	0·535	0·556	1·400	1·420	0·470	1·397	0·382	0·392
22	0·513	0·555	1·378	1·420	0·408	1·265	0·373	0·391
17	0·529	0·554	1·394	1·418	0·352	0·989	0·380	0·390
338	0·523	0·538	1·387	1·402	0·419	0·731	0·377	0·383
57	0·529	0·542	1·393	1·407	0·336	0·949	0·380	0·385
Ice II (*e*) (I)	0·573		1·435			2·73	0·40	
(II)		0·620		1·485	0·742			0·42
Ice IX (*e*) (I)		0·569		1·430		2·55		0·40
(II)	0·557		1·414		0		0·39	

(*a*) The dipole vectors, μ, are in a.u. with conversion factors of 2.541 765 (D/a.u.) and $8{\cdot}478\,418\times10^{-30}$ (C m/a.u.). The permanent, induced and total dipole vectors are denoted by μ_{perm}, μ_{ind}, $\mu_{\mathrm{tot}}=\mu_{\mathrm{perm}}+\mu_{\mathrm{ind}}$. (*b*) $\theta\equiv$ the angle between μ_{tot} and μ_{perm} in degrees. (*c*) The columns headed Min (Max) give the least (greatest) value of the specified variable. (*d*) The ten configurations, specified by the configuration numbers in column 1, for Ice Ih were chosen as representatives from each of the ten classes with a zero net dipole vector. They are defined in table 5 of Appendix 2. (*e*) The superscripts specify the lattice site type. The symbols I and II are defined in §§ 2.3, 2.4. (*f*) The Ih values are for $r_0=2{\cdot}741$ Å.

The quantitative effect of the error in the wave function is difficult to assess because of varying quality of the moments it defines. Thus the permanent quadrupole components for this wave function agree well with both those defined by the largest gaussian type orbital functions of [71]† (PKC[3] $Q^{11}=-5{\cdot}716$, $Q^{22}=-4{\cdot}171$, $Q^{33}=-7{\cdot}493$; NM[71] $Q^{11}=-5{\cdot}708$, $Q^{22}=-4{\cdot}180$, $Q^{33}=-7{\cdot}482$) and with the experimental values of [72] (PKC[3] $\theta^{11}=-0{\cdot}028$, $\theta^{22}=+2{\cdot}506$, $\theta^{33}=-2{\cdot}478$; exp $\theta^{11}=-0{\cdot}13$, $\theta^{22}=+2{\cdot}63$, $\theta^{33}=-2.50$)†. (For this comparison, Buckingham's convention [7] has been adopted in which

$$\theta^{ij}\equiv\left(3Q^{ij}-\delta^{ij}\sum_{k=1}^{3}Q^{kk}\right)\Big/2,$$

and the expansion centre has been translated to the centre of mass.) Conversely, the calculated dipole moment of 2·197 D shows an 18 per cent error in comparison with the experimental value of $1{\cdot}8546\pm0{\cdot}0004$ D [73]‡.

The following argument reduces the average over classes for the total (induced) dipole moment in Ih from 3·588 (1·390) to 2·94 (1·089) D after correction for errors in **E** arising from the wave function assumed for water: (i) To a first approximation, one might expect that the contribution of higher order multipoles to **E** increases as **E** increases. (ii) Since by tables 2 and 3 **E**, $\boldsymbol{\mu}_{\text{perm}}$ and $\boldsymbol{\mu}_{\text{ind}}$ are approximately collinear, the non-cooperative contribution (cooperative correction) to $\boldsymbol{\mu}_{\text{ind}}$ should scale approximately as $\|\mathbf{E}\|$, and, therefore, as $\|\boldsymbol{\mu}_{\text{tot}}\|$ of the model assumed (multiplied by $(1-(\Delta\|\boldsymbol{\mu}_{\text{ind}}\|)/\|\boldsymbol{\mu}_{\text{tot}}\|)$ where Δ is the non-cooperative correction). These values can be compared with Coulson and Eisenberg's [74] values, 2·60 D and 0·82 D. Although they also report a ratio $\|\boldsymbol{\mu}_{\text{induced}}\|/\|\boldsymbol{\mu}_{\text{total}}\|=0{\cdot}315$, compared with the average of our data in table 3, 0·388, the averages smooth out important differences. (Their total dipole moment is the average of values ranging from 1·9 to 3·1 D whereas the calculations reported here show that the variation is $<4{\cdot}2$ (5·6 per cent) for the set of 10 (55) classes, respectively). Finally, the value for total moment can be compared with the estimate of 2·3 D obtained from the Onsager reaction field for the model of a single point dipole at the centre of a sphere of molecular size in a dielectric continuum [75 (*a*)].

We express our appreciation to the National Institutes of Health which supported this work under Grant 1R01 GM20436-02.

Appendix 1

Extrapolations for r_0 (0 K)

Four different extrapolations of the nearest neighbour O–O distance, r_0, were made. (i) Extrapolation of Barnes' [22] data gave a value used in earlier calculations, r_0 (0 K) = 2·72 Å [35 (*b*)]. (ii) Integration of Dantl's [76] data on thermal expansion gave a better estimate, r_0 (0 K) = $2{\cdot}74_4$ Å [35 (*b*)]. However, others [24] found no evidence of negative coefficients of thermal expansion at lower temperatures such as he reported and are found in some tetrahedral

† The units are 10^{26} esu cm^2. The moments in frames (9) were calculated relative to the O nucleus using the definitions of [9] using the wave functions of the cited references.

‡ The conversion factors are $3{\cdot}335\,641\times10^{-14}$ C m^2/esu cm^2 and $3{\cdot}335\,641\times10^{-30}$ C m/D.

lattices [30 (*b*)]. (iii) La Placa and Post's [23] data on $\mathbf{a}'_1=\mathbf{a}'_2$ are anomalous, non-monotone functions of temperature over $[-100°, -130°]$ and are, therefore, not suitable for extrapolation. Moreover, if the O–O–O angles were tetrahedral, their ratio $\|\mathbf{a}'_3\|/\|\mathbf{a}'_1\| < (8/3)^{1/2}$ would imply $\|O_1 \rightarrow O_3\| > \|O_1 \rightarrow O_4\|$, whereas Chamberlain, Moore and Fletcher's [19] best estimate is that $\|O_1 \rightarrow O_4\| > \|O_1 \rightarrow O_3\|$. However, their values for $\|\mathbf{a}'_3\|$ are monotone and are in general agreement with the data of [24]. To test the possibility of combining their values for $\|\mathbf{a}'_3\|$ with the assumption of ideal geometry of § 2.2, we extrapolated their data to 77 K to obtain r^0 (77 K) = $2{\cdot}744_1$ Å in agreement with the best estimate of Chamberlain, Moore and Fletcher [19], 2·744 Å. This agreement is a result of the fact that the increase in the $\mathbf{a}'_3$ component of $(O_3 \rightarrow O_1)$ arising from the amount their O_3–O_1–O_4 angle exceeds the ideal tetrahedral value of $(8/3)^{1/2}$ almost exactly balances the amount by which $(O_1 \rightarrow O_3)$ is shorter than $(O_1 \rightarrow O_4)$. Therefore, La Placa and Post's data on $\|\mathbf{a}'_3\|$ were extrapolated to 0 K and the ideal geometry was assumed to obtain r_0 (0 K) = $2{\cdot}74_{07}$ Å. (iv) The extrapolation of Brill and Tippe's [24] $\|\mathbf{a}'_3\|$ at 13 K to 0 K yields a correction of only 0·0001 Å. Assumption of the ideal geometry of § 2.2 then gives r_0 (0 K) = $2{\cdot}74_{49}$ Å.

Appendix 2

Possible orientations for water molecules in ice Ih

Let O^c be any oxygen site of the lattice at the geometric centre of four nearest neighbour sites, O^n, $n=1, \ldots, 4$. The possible orientations for the central H_2O consistent with Pauling's rules given by (4) are defined by specifying for each of the two H of the central molecule the particular O^n, such that $O^c \rightarrow H$ lies approximately along $O^c \rightarrow O^n$. Define an orthogonal system:

$$\mathbf{e}_3=\mathbf{a}'_3/\|\mathbf{a}'_3\|, \quad \mathbf{e}_1=\mathbf{a}'_1/\|\mathbf{a}'_1\|, \quad \mathbf{e}_2=\mathbf{e}_3\times\mathbf{e}_1. \tag{A 2.1}$$

Let:

δ: the sole $O^c \rightarrow O^n$ which has zero $\mathbf{e}_1$ and $\mathbf{e}_2$ components; α: the $O^c \rightarrow O^n$ which has a negative $\mathbf{e}_1$ component; β: the $O^c \rightarrow O^n$ which has a positive $\mathbf{e}_1$ component; γ: the $O^c \rightarrow O^n$ which has a zero $\mathbf{e}_1$ and a non-zero $\mathbf{e}_2$ component. (A 2.2)

Table 4. Possible dipole directions, **s**, and orientations for water molecules in ice Ih.

Positions (i)										
(*a*)		(*b*)		(*c*)		(*d*)		**s**		
VP (ii)	DI (ii)	VP	DI	VP	DI	VP	DI	s_1	s_2	s_3 (iii)
αβ	1	γδ	12	αβ	13	γδ	24	0	$-(2/3)^{1/2}$	$\pm(1/3)^{1/2}$
αγ	2	αδ	11	αγ	14	αδ	23	$-(1/2)^{1/2}$	$+(1/6)^{1/2}$	$\pm(1/3)^{1/2}$
αδ	3	αγ	10	αδ	15	αγ	22	$-(1/2)^{1/2}$	$-(1/6)^{1/2}$	$\pm(1/3)^{1/2}$
βγ	4	βδ	9	βγ	16	βδ	21	$+(1/2)^{1/2}$	$+(1/6)^{1/2}$	$\pm(1/3)^{1/2}$
βδ	5	βγ	8	βδ	17	βγ	20	$+(1/2)^{1/2}$	$-(1/6)^{1/2}$	$\pm(1/3)^{1/2}$
γδ	6	αβ	7	γδ	18	αβ	19	0	$+(2/3)^{1/2}$	$\pm(1/3)^{1/2}$

(i) The positions are defined by (3). (ii) VP, vector pair; DI, dipole index. (iii) The upper sign applies to (*a*) and (*b*) positions. Thus, s_3 is negative for indices 1 and 12 and positive for indices 13 and 24.

Table 5. Orientations for a representative from each energy class for which the net dipole vector vanishes.

		Dipole indices (*c*)															
N_E	N_c	z_{000} (*d*)				z_{100}				z_{010}				z_{110}			
(*a*)	(*b*)	*a*	*b*	*c*	*d*	*a*	*b*	*c*	*d*	*a*	*b*	*c*	*d*	*a*	*b*	*c*	*d*
1	412	3	7	16	24	4	12	15	19	4	12	15	19	3	7	16	24
2	329	6	7	13	24	5	9	14	22	2	7	17	24	4	12	15	19
4	352	6	7	13	24	5	8	14	23	2	11	17	20	1	12	18	19
7	363	6	7	13	24	4	9	15	22	4	9	15	22	6	7	13	24
8	108	2	7	18	23	5	12	13	20	2	7	18	23	5	12	13	20
11	326	6	7	13	24	4	9	15	22	2	7	17	24	6	11	13	20
16	22	3	7	14	23	4	12	15	22	4	8	18	23	5	9	13	20
24	17	3	7	14	23	4	12	15	22	6	10	16	21	1	9	17	20
30	338	6	7	13	24	4	9	15	22	6	7	13	24	4	9	15	22
32	57	6	7	14	23	5	8	13	24	2	11	18	19	1	12	17	20

(*a*) The energy classes N_E are defined in equation (30 *b*), p. 2698 of [35]. (*b*) The configuration numbers N_c are given for reference to the thesis of Gelernter (1965, Ph.D. Thesis, New York University). (*c*) The dipole indices are defined by table 4. (*d*) The unit cells z_{ijk} are defined by (5).

The possible dipole directions and the indexing which simplifies the discussion results is given by table 4. Table 5 gives the dipole indices of table 4 for one representative from each of ten energy classes whose members have zero net dipole vectors for the unit cells.

Appendix 3

Sites and orientations in ice IX

The coordinates given in table 6 for the twelve water molecules were derived as follows. The fractional unit cell coordinates for the O atom of each type have been reported from both neutron diffraction [17] and from X-ray diffraction experiments [41]. Since slightly smaller error limits were assigned to the values from neutron diffraction, the latter were adopted. The O site coordinates were then calculated using the unit cell constants given by (6), the general transformations for eight equivalent sites of no point symmetry for O(I) type sites and the transformations for four equivalent sites on a twofold axis for O(II) type sites. Whereas the two deuterium sites for O(I) type O atoms were determined in the same way as the O(I) positions, the values for O(II) type positions were derived as follows. The O(II) is on a symmetry axis such that the coordinates given for one D atom $\langle a, b, c\rangle$ yield the coordinates $\langle b, a, -c\rangle$ for the other. Since the D atoms are not themselves on the twofold axis, the coordinates for the remaining three molecules were generated by applying the general transformations for sites of no point symmetry.

The orientations of the water molecules are such that each $O(I, j)$ has the four nearest-neighbours, $[O(I, j^{i}), O(I, j^{ii}), O(II, j^{iii}), O(II, j^{iv})]$, and each $O(II, j)$ the four $[O(I, j^{i}), O(I, j^{ii}), O(I, j^{iii}), O(I, j^{iv})]$. Table 7 identifies

Table 6. Coordinates for the sites in the unit cell of ice IX.

	c_1	c_2	c_3
O(I, 1)	0·734 916	2·029 095	1·952 014
D_α(I, 1)	−0·083 452	2·235 033	1·459 571
D_β(I, 1)	0·765 874	1·061 321	2·027 144
O(I, 2)	2·029 095	0·734 916	−1·952 014
D_α(I, 2)	2·235 033	−0·083 452	−1·459 571
D_β(I, 2)	1·061 321	0·765 874	−2·027 144
O(I, 3)	−0·734 916	−2·029 095	5·367 014
D_α(I, 3)	0·083 452	−2·235 033	4·874 571
D_β(I, 3)	−0·765 874	−1·061 321	5·442 144
O(I, 4)	−2·029 095	−0·734 916	1·462 986
D_α(I, 4)	−2·235 033	0·083 452	1·955 429
D_β(I, 4)	−1·061 321	−0·765 874	1·387 856
O(I, 5)	1·335 905	4·099 916	3·659 514
D_α(I, 5)	1·129 967	3·281 548	3·167 071
D_β(I, 5)	2·303 679	4·130 874	3·734 644
O(I, 6)	2·630 084	5·394 095	−0·244 514
D_α(I, 6)	3·448 452	5·600 033	0·247 929
D_β(I, 6)	2·599 126	4·426 321	−0·319 644
O(I, 7)	5·394 095	2·630 084	7·074 514
D_α(I, 7)	5·600 033	3·448 452	6·582 071
D_β(I, 7)	4·426 321	2·599 126	7·149 644
O(I, 8)	4·099 916	1·335 905	3·170 486
D_α(I, 8)	3·281 548	1·129 967	3·662 929
D_β(I, 8)	4·130 874	2·303 679	3·095 356
O(II, 9)	2·642 198	2·642 198	0·0
D_α(II, 9)	2·020 346	2·418 762	0·721 931
D_β(II, 9)	2·418 762	2·020 346	−0·721 931
O(II, 10)	−2·642 198	−2·642 198	3·415 000
D_α(II, 10)	−2·020 346	−2·418 762	4·136 931
D_β(II, 10)	−2·418 762	−2·040 346	2·693 069
O(II, 11)	0·722 802	6·007 198	1·707 500
D_α(II, 11)	0.946 238	5·385 346	2·429 431
D_β(II, 11)	1·344 654	5·783 762	0·985 569
O(II, 12)	6·007 198	0·722 802	5·122 500
D_α(II, 12)	5·783 762	1·344 654	5·844 431
D_β(II, 12)	5·385 346	0·946 238	4·400 569

Each site is at $\sum_{i=1}^{3} c_i \mathbf{e}_i$ Å where $\mathbf{e}_i = \mathbf{a}_i / \|\mathbf{a}_i\|$ and $\|\mathbf{a}_1\| = \|\mathbf{a}_2\| = 6{\cdot}73$ Å, $\|\mathbf{a}_3\| = 6{\cdot}83$ Å, and 1 Å $= 10^{-10}$ m. The types of the oxygen sites I, II are defined following (6). In the notation of [17], $D_\alpha(\kappa, j)$ is a D_5 site for $O(\kappa, j)$, $\kappa =$ I, and $D_\beta(\kappa, j)$ is a D_6 site for $\kappa =$ I. For $\kappa =$ II, both α and β are D_7 sites.

for each water molecule in the unit cell the two nearest neighbours to which it donates a proton to form an H–bond and the two from which it accepts a proton.

Table 7. Sets of nearest neighbours for all O-sites and the hydrogen bonding in the unit cell $\langle 0, 0, 0\rangle$ of ice IX.

Unit cell sites	$\langle j, n_1, n_2, n_3\rangle$ $\mathscr{D}_\alpha$	$\mathscr{D}_\beta$	$\mathscr{A}_\alpha$	$\mathscr{A}_\beta$
O(I, 1)	$\langle 7, -1, 0, -1\rangle$	$\langle 11, 0, -1, 0\rangle$	$\langle 5, 0, 0, 0\rangle$	$\langle 9, 0, 0, 0\rangle$
O(I, 2)	$\langle 6, 0, -1, 0\rangle$	$\langle 12, -1, 0, -1\rangle$	$\langle 8, 0, 0, -1\rangle$	$\langle 9, 0, 0, 0\rangle$
O(I, 3)	$\langle 5, 0, -1, 0\rangle$	$\langle 12, -1, 0, 0\rangle$	$\langle 7, -1, -1, 0\rangle$	$\langle 10, 0, 0, 0\rangle$
O(I, 4)	$\langle 8, -1, 0, 0\rangle$	$\langle 11, 0, -1, 0\rangle$	$\langle 6, -1, -1, 0\rangle$	$\langle 10, 0, 0, 0\rangle$
O(I, 5)	$\langle 1, 0, 0, 0\rangle$	$\langle 10, 1, 1, 0\rangle$	$\langle 3, 0, 1, 0\rangle$	$\langle 11, 0, 0, 0\rangle$
O(I, 6)	$\langle 4, 1, 1, 0\rangle$	$\langle 9, 0, 0, 0\rangle$	$\langle 2, 0, 1, 0\rangle$	$\langle 11, 0, 0, 0\rangle$
O(I, 7)	$\langle 3, 1, 1, 0\rangle$	$\langle 9, 0, 0, 1\rangle$	$\langle 1, 1, 0, 1\rangle$	$\langle 12, 0, 0, 0\rangle$
O(I, 8)	$\langle 2, 0, 0, 1\rangle$	$\langle 10, 1, -1, 0\rangle$	$\langle 4, 1, 0, 0\rangle$	$\langle 12, 0, 0, 0\rangle$
O(II, 9)	$\langle 1, 0, 0, 0\rangle$	$\langle 2, 0, 0, 0\rangle$	$\langle 6, 0, 0, 0\rangle$	$\langle 7, 0, 0, -1\rangle$
O(II, 10)	$\langle 3, 0, 0, 0\rangle$	$\langle 4, 0, 0, 0\rangle$	$\langle 5, -1, -1, 0\rangle$	$\langle 8, -1, 1, 0\rangle$
O(II, 11)	$\langle 5, 0, 0, 0\rangle$	$\langle 6, 0, 0, 0\rangle$	$\langle 1, 0, 1, 0\rangle$	$\langle 4, 0, 1, 0\rangle$
O(II, 12)	$\langle 7, 0, 0, 0\rangle$	$\langle 8, 0, 0, 0\rangle$	$\langle 2, 1, 0, 1\rangle$	$\langle 3, 1, 0, 0\rangle$

In each ordered 4-tuple, the first index j selects a particular O(I, j) when $1 \leqslant j \leqslant 8$ and an O(II, j) when $9 \leqslant j \leqslant 12$. The last three indices select the unit cell so that the nearest neighbour is located $\mathbf{r}[\mathrm{O}(\kappa, j)] + \sum_{i=1}^{3} n_i \mathbf{a}_i$, $\kappa = \mathrm{I}, \mathrm{II}$, and the $\mathbf{a}_i$ are the unit cell axis vectors. The columns headed by $\mathscr{D}_\alpha$ and $\mathscr{D}_\beta$ give the two nearest neighbours to which the unit cell water donates hydrogens α and β. In the notation of [17]: for O(I, j), $\mathscr{D}_\alpha$ is a D_5 type site and $\mathscr{D}_\beta$ is a D_6 type site; for O(II, j), both are D_7 types sites. The columns headed $\mathscr{A}_\alpha$ and $\mathscr{A}_\beta$ give the nearest neighbours from which it accepts a hydrogen. In the notation of [17]: for O(I, j), $\mathscr{A}_\alpha$ accepts a D_5 type site hydrogen and $\mathscr{A}_\beta$ a D_7 type site hydrogen; for O(II, j), both $\mathscr{A}_\alpha$ and $\mathscr{A}_\beta$ accept D_6 type site hydrogens.

Appendix 4

Sites and orientations in ice II

Since only approximate H atom coordinates could be inferred from single crystal X-ray diffraction of $H_2O(s)$ [43], the coordinates from neutron diffraction of $D_2O(s)$ [16] were adopted in these calculations. Comparison of the trial (cf. p. 1937) with the refined coordinates (cf. p. 1938) for oxygen sites indicated a printing error for those of the O(II) site that also occurred in the earlier paper. This was verified by comparing the computed with published atom–atom distances. The correct fractional unit cell coordinates for the O(II) site are the following permutation of those given: $\langle 0{\cdot}7571, 0{\cdot}3389, 0{\cdot}4798\rangle$. The computational algorithm assumes an orthogonal system which was defined as follows. Let: $\{\mathbf{e}_i\}$, $\{\mathbf{e}_i^{\mathrm{R}}\}$, $\{\mathbf{e}_i^{\mathrm{H}}\}$: the sets of unit basis vectors for the new orthogonal system, the rhombohedral unit cell of $R_{\bar{3}}$, and the alternative hexagonal system. Then, $\mathbf{e}_1 \equiv \mathbf{e}_1^{\mathrm{H}}$, $\mathbf{e}_3 \equiv \mathbf{e}_3^{\mathrm{H}}$ and $\mathbf{e}_2 = \mathbf{e}_3 \times \mathbf{e}_1$. Thus the counterclockwise angle from $\mathbf{e}_2$ to $\mathbf{e}_2^{\mathrm{H}}$ is $+\pi/6$. Let the transformation matrix between the rhombohedral and orthogonal systems be defined as

Table 8. Orthogonal coordinates for the sites in the rhombohedral unit cell.

	c_1	c_2	c_3
O(I, 1)	1·594 931	2·217 572	0·313 484
D_2(I, 1)	0·700 420	2·229 565	−0·025 012
D_4(I, 1)	1·478 736	2·441 316	1·255 185
O(I, 2)	−2·717 939	0·272 465	0·313 484
D_2(I, 2)	−2·281 070	−0·508 201	−0·025 012
D_4(I, 2)	−2·853 609	0·059 965	1·255 185
O(I, 3)	1·123 008	−2·490 037	0·313 484
D_2(I, 3)	1·580 650	−1·721 364	−0·025 012
D_4(I, 3)	1·374 874	−2·501 280	1·255 185
O(I, 4)	−1·594 931	−2·217 572	−0·313 484
D_2(I, 4)	−0·700 420	−2·229 565	0·025 012
D_4(I, 4)	−1·478 736	−2·441 316	−1·255 185
O(I, 5)	2·717 939	−0·272 465	−0·313 484
D_2(I, 5)	2·281 070	0·508 201	0·025 012
D_4(I, 5)	2·853 609	−0·059 965	−1·255 185
O(I, 6)	−1·123 008	2·490 037	−0·313 484
D_2(I, 6)	−1·580 650	1·721 364	0·025 012
D_4(I, 6)	−1·347 874	2·501 280	−1·255 185
O(II, 7)	2·714 694	0·511 200	3·284 491
D_1(II, 7)	2·107 101	1·219 533	3·200 701
D_3(II, 7)	3·532 607	0·742 814	2·731 726
O(II, 8)	−1·800 059	2·095 394	3·284 491
D_1(II, 8)	−2·109 697	1·215 036	3·200 701
D_3(II, 8)	−2·409 599	2·687 921	2·731 726
O(II, 9)	−0·914 635	−2·606 593	3·284 491
D_1(II, 9)	0·002 597	−2·434 570	3·200 701
D_3(II, 9)	−1·123 008	−3·430 734	2·731 726
O(II, 10)	−2·714 694	−0·511 200	−3·284 491
D_1(II, 10)	−2·107 101	−1·219 533	−3.200 701
D_3(II, 10)	−3·532 607	−0·742 814	−2·731 726
O(II, 11)	1·800 059	−2·095 394	−3·284 491
D_1(II, 11)	2·109 697	−1·215 036	−3·200 701
D_3(II, 11)	2·409 599	−2·687 921	−2·731 726
O(II, 12)	0·914 635	2·606 593	−3·284 491
D_1(II, 12)	−0·002 597	2·434 570	−3·200 701
D_3(II, 12)	1·123 008	3·430 734	−2·731 726

Each site is at $\sum_{i=1}^{3} c_i \mathbf{e}_i$ where the basis vectors are defined above, and the distances are in Å. The types of the oxygen sites I, II are defined following (7). The subscripts on D identify the O sites following the convention of [16].

Table 9. Sets of nearest-neighbours for all O-sites and the hydrogen bonding in the unit cell $\langle 0, 0, 0\rangle$ of ice II.

Unit cell sites	$\langle j, n_1, n_2, n_3\rangle$ $\mathscr{D}_\alpha$	$\mathscr{D}_\beta$	$\mathscr{A}_\alpha$	$\mathscr{A}_\beta$
O(I, 1)	$\langle 6, 0, 0, 0\rangle$	$\langle 12, 1, 1, 1\rangle$	$\langle 5, 0, 0, 0\rangle$	$\langle 10, 1, 0, 0\rangle$
O(I, 2)	$\langle 4, 0, 0, 0\rangle$	$\langle 10, 1, 1, 1\rangle$	$\langle 6, 0, 0, 0\rangle$	$\langle 11, 0, 1, 0\rangle$
O(I, 3)	$\langle 5, 0, 0, 0\rangle$	$\langle 11, 1, 1, 1\rangle$	$\langle 4, 0, 0, 0\rangle$	$\langle 12, 0, 0, 1\rangle$
O(I, 4)	$\langle 3, 0, 0, 0\rangle$	$\langle 9, -1, -1, -1\rangle$	$\langle 2, 0, 0, 0\rangle$	$\langle 7, -1, 0, 0\rangle$
O(I, 5)	$\langle 1, 0, 0, 0\rangle$	$\langle 7, -1, -1, -1\rangle$	$\langle 3, 0, 0, 0\rangle$	$\langle 8, 0, -1, 0\rangle$
O(I, 6)	$\langle 2, 0, 0, 0\rangle$	$\langle 8, -1, -1, -1\rangle$	$\langle 1, 0, 0, 0\rangle$	$\langle 9, 0, 0, -1\rangle$
O(II, 7)	$\langle 12, 1, 1, 1\rangle$	$\langle 4, 1, 0, 0\rangle$	$\langle 11, 1, 1, 1\rangle$	$\langle 5, 1, 1, 1\rangle$
O(II, 8)	$\langle 10, 1, 1, 1\rangle$	$\langle 5, 0, 1, 0\rangle$	$\langle 12, 1, 1, 1\rangle$	$\langle 6, 1, 1, 1\rangle$
O(II, 9)	$\langle 11, 1, 1, 1\rangle$	$\langle 6, 0, 0, 1\rangle$	$\langle 10, 1, 1, 1\rangle$	$\langle 4, 1, 1, 1\rangle$
O(II, 10)	$\langle 9, -1, -1, -1\rangle$	$\langle 1, -1, 0, 0\rangle$	$\langle 8, -1, -1, -1\rangle$	$\langle 2, -1, -1, -1\rangle$
O(II, 11)	$\langle 7, -1, -1, -1\rangle$	$\langle 2, 0, -1, 0\rangle$	$\langle 9, -1, -1, -1\rangle$	$\langle 3, -1, -1, -1\rangle$
O(II, 12)	$\langle 8, -1, -1, -1\rangle$	$\langle 3, 0, 0, -1\rangle$	$\langle 7, -1, -1, -1\rangle$	$\langle 1, -1, -1, -1\rangle$

In each ordered 4-tuple, the first index j selects a particular O(I, j) when $1 \leqslant j \leqslant 6$ and an O(II, j) when $7 \leqslant j \leqslant 12$. The indices n_i select the unit cell so that the nearest neighbour is located at $\mathbf{r}[\mathrm{O}(\kappa, j)] + \sum_{i=1}^{3} n_i \mathbf{a}_i$, $\kappa = \mathrm{I}, \mathrm{II}$ and the $\mathbf{a}_i$ are the rhombohedral unit cell basis vectors. The columns headed by $\mathscr{D}_\alpha$ and $\mathscr{D}_\beta$ give the two nearest neighbours to which the unit cell water donates a hydrogen and the columns headed by $\mathscr{A}_\alpha$ and $\mathscr{A}_\beta$ the nearest neighbours from which it accepts a proton. For $j = 1, 6$ ($\alpha = 2$, $\beta = 4$), for $j = 7, 12$ ($\alpha = 1$, $\beta = 3$). These values are in the notation of [16].

follows :

$$(\mathbf{e}_1^{\mathrm{R}}, \mathbf{e}_2^{\mathrm{R}}, \mathbf{e}_3^{\mathrm{R}}) = (\mathbf{e}_1, \mathbf{e}_2, \mathbf{e}_3)\mathrm{M} \leftrightarrow \begin{bmatrix} x_1 \\ x_2 \\ x_3 \end{bmatrix} = \mathrm{M} \begin{bmatrix} x_1^{\mathrm{R}} \\ x_2^{\mathrm{R}} \\ x_3^{\mathrm{R}} \end{bmatrix}; \qquad \text{(A 4.1)}$$

$$\mathrm{M} = \begin{pmatrix} \sin(\alpha/2) & (3)^{-1/2}\sin(\alpha/2) & [(1+2\cos\alpha)/3]^{1/2} \\ -\sin(\alpha/2) & (3)^{-1/2}\sin(\alpha/2) & [(1+2\cos\alpha)/3]^{1/2} \\ 0 & -2(3)^{-1/2}\sin(\alpha/2) & [(1+2\cos\alpha)/3]^{1/2} \end{pmatrix}; \qquad \text{(A 4.2)}$$

α : the rhombohedral angle given by (7). (A 4.3)

The coordinates for the orthogonal system, which are recorded in table 8 for the O sites were obtained using the unit cell constants given by (7), the corrected fractional rhombohedral coordinates (*vide supra*) and the above transformation. The coordinates for the H sites were calculated according to the discussion following (7).

The orientations of the water molecules are such that each O(I, j) and each O(II, j) has four nearest neighbours : O(I, j) : O(I, j^{i}), O(II, j^{ii}), O(I, j^{iii}),

$O(II, j^{iv})$; $O(II, j)$: $O(II, j^{i})$, $O(I, j^{ii})$, $O(II, j^{iii})$, $O(I, j^{iv})$. Table 9 identifies for each water molecule in the rhombohedral unit cell the two nearest neighbours to which it donates a proton to form an H–bond and the two from which it accepts a proton.

Appendix 5

Some energetic consequences of a polar structure

Consider the potential defined by a set of parallel dipoles at the sites of an orthogonal simple translation lattice. Although it is well known that the partial sums for those sites contained within an expanding sequence of concentric spheres converge, it has been shown that : (i) the partial sums diverge for the Ewald summation order ; (ii) for a union of such simple translation lattices, the necessary and sufficient condition that the partial sums converge for the Ewald summation order is that the net unit cell dipole vector vanish [34 (*a*)]. This implies that the potentials for such finite polar lattices are shape dependent. It is plausible to assume that the same conclusions would be valid for arbitrary non-orthogonal crystal axes. Any such structure for a real crystal would lead to stabilization by absorption of ions from the atmosphere and the r^{-2} dependence of ion–dipole energies should lead to a contribution to the specific energy of such a crystal ; (iii) the partial sums for the energy of interaction between a fixed dipole and a set of dipoles at the sites of a simple translation lattice converge for the summation order defined by growth of the crystal along its axes (the summation order implicitly assumed by the Ewald formulae). However, similar arguments to those used in Appendix C in that article show that the convergence for a crystal whose simple translation lattices define a unit cell with a vanishing net dipole is considerably more rapid. In this case, the expected dependence of the limit given by crystal growth defined by alternative shapes to growth along the crystal axes should be less important.

References

[1] Campbell, E. S., and Mezei, M., 1977, *J. chem. Phys.*, **67,** 2338 ; (*a*) cf. p. 2339 and [13].
[2] Campbell, E. S., and Belford, D. (submitted for publication).
[3] Popkie, H., Kistenmacher, H., and Clementi, E., 1973, *J. chem. Phys.*, **59,** 1325.
[4] Kistenmacher, H., Lie, G. C., Popkie, H., and Clementi, E., 1974, *J. chem. Phys.*, **61,** 546.
[5] Hankins, D., Moskowitz, J. W., and Stillinger, F. H., 1970, *J. chem. Phys.*, **53,** 4544 ; erratum, 1973, *Ibid.*, **59,** 995.
[6] Mezei, M., and Campbell, E. S., 1977, *Theor. chim. Acta*, **43,** 227 ; (*a*) Appendices A, B.
[7] Buckingham, A. D., 1959, *Q. Rev. chem. Soc.*, **13,** 183.
[8] Campbell, E. S., and Mezei, M. (submitted for publication).
[9] Mezei, M., and Campbell, E. S., 1976, *J. comput. Phys.*, **20,** 110.
[10] Campbell, E. S., and Mezei, M., 1976, *J. comput. Phys.*, **21,** 114.
[11] Campbell, E. S., 1965, *J. Phys. Chem. Solids*, **26,** 1395 ; (*a*) Equations (23), (39), (40).
[12] Mezei, M., and Campbell, E. S., 1978, *J. comput. Phys.*, **29,** 297.
[13] Campbell, E. S., 1967, *Helv. phys. Acta*, **40,** 387.
[14] Jeziorski, B., and van Hemert, M., 1976, *Molec. Phys.*, **31,** 713.
[15] Benedict, W. S., Gailar, N., and Plyler, E. K., 1956, *J. chem. Phys.*, **24,** 1139.

[16] KAMB, B. HAMILTON, W. C., LA PLACA, S. J., and PRAKASH, A., 1971, *J. chem. Phys.*, **55,** 1934.
[17] LA PLACA, S. J., HAMILTON, W. C., KAMB, B., and PRAKASH, A., 1973, *J. chem. Phys.*, **58,** 567 ; (*a*) p. 578.
[18] PETERSEN, S. W., and LEVY, H. A., 1957, *Acta crystallogr.*, **10,** 70.
[19] CHAMBERLAIN, J. S., MOORE, F. H., and FLETCHER, N. H., 1973, *Physics and Chemistry of Ice*, edited by E. Whalley, S. J. Jones and L. W. Gold (University of Toronto Press), p. 283 ; (*a*) p. 284.
[20] WALFORD, G., CLARKE, J. H., and DORE, J. C., 1977, *Molec. Phys.*, **33,** 25.
[21] WHALLEY, E., 1974, *Molec. Phys.*, **28,** 1105.
[22] BARNES, W. H., 1929, *Proc. R. Soc.* A, **125,** 670.
[23] LA PLACA, S. J., and POST, B., 1960, *Acta crystallogr.*, **13,** 503.
[24] BRILL, R., and TIPPE, A., 1967, *Acta crystallogr.*, **23,** 343.
[25] HANDLER, E. S., 1968, Thesis in partial fulfilment of the requirements for the Ph.D., Polytechnic Institute of Brooklyn, (*a*) p. 79.
[26] SCHERER, J. R., and SNYDER, R. G., 1977, *J. chem. Phys.*, **67,** 4794.
[27] PAULING, L., 1935, *J. Am. chem. Soc.*, **57,** 2680.
[28] GIAUQUE, W. F., and STOUT, J. W., 1936, *J. Am. chem. Soc.*, **58,** 1144.
[29] NAGLE, J. F., 1966, *J. math. Phys.*, **7,** 1484.
[30] KAMB, B., 1973, *Physics and Chemistry of Ice*, edited by E. Whalley, S. J. Jones and L. W. Gold (University of Toronto Press), p. 28 ; (*a*) p. 39 ; (*b*) p. 37.
[31] JOHARI, G. P., and WHALLEY, E., 1973, *Physics and Chemistry of Ice*, edited by E. Whalley, S. J. Jones and L. W. Gold (University of Toronto Press), p. 278.
[32] JOHARI, G. P., and JONES, S. J., 1975, *J. chem. Phys.*, **62,** 4213.
[33] JOHARI, G. P., and JONES, S. J., 1976, *Proc. R. Soc.* A, **349,** 467 ; cf. p. 487.
[34] CAMPBELL, E. S. 1963, *J. Phys. Chem. Solids*, **24,** 197 ; (*a*) p. 203, Appendices B, C.
[35] CAMPBELL, E. S., GELERNTER, G., HEINEN, H., and MOORTI, V. R. G., 1967, *J. chem. Phys.*, **46,** 2690 ; (*a*) p. 2698 ; (*b*) p. 2694 ; (*c*) table III, p. 2700 ; (*d*) table II, p. 2699.
[36] WILSON, G. J., CHAN, R. K., DAVIDSON, D. W., and WHALLEY, E., 1965, *J. chem. Phys.*, **43,** 2384 ; (*a*) p. 2390.
[37] WHALLEY, E., HEATH, J. B. R., and DAVIDSON, D. W., 1968, *J. chem. Phys.*, **48,** 2362 ; (*a*) p. 2366.
[38] BERTIE, J. E., and WHALLEY, E., 1964, *J. chem. Phys.*, **40,** 1646.
[39] KELL, G. S., and WHALLEY, E., 1968, *J. chem. Phys.*, **48,** 2359.
[40] NISHIBATA, K., and WHALLEY, E., 1974, *J. chem. Phys.*, **60,** 3189.
[41] KAMB, B., and PRAKASH, A., 1968, *Acta crystallogr.* B, **24,** 1317.
[42] ARNOLD, G. P., WENZEL, R. G., RABIDEAU, S. W., NERESON, N. G., and BOWMAN, A. L., 1971, *J. chem. Phys.*, **55,** 589 ; (*a*) p. 594.
[43] KAMB, B., 1964, *Acta crystallogr.*, **17,** 1437 ; (*a*) p. 1446 ; (*b*) p. 1438.
[44] LIEBMANN, S. P., and MOSKOWITZ, J. W., 1971, *J. chem. Phys.*, **54,** 3622.
[45] JASZUNSKI, M., AKNINSKI, A., and SADLEJ, A. J., 1972, *Acta phys. pol.* A, **41,** 595.
[46] WERNER, H. J., and MEYER, W., 1976, *Molec. Phys.*, **31,** 855 ; (*a*) p. 870.
[47] MURPHEY, W. F., 1978, *J. chem. Phys.*, **67,** 5877.
[48] RAHMAN, A., and STILLINGER, F. H., 1972, *J. chem. Phys.*, **57,** 4009.
[49] EISENBERG, D., and KAUZMANN, W., 1969, *The Structure and Properties of Water* (Oxford University Press) ; (*a*) p. 93 ; (*b*) p. 95.
[50] WHALLEY, E., 1973, *Physics and Chemistry of Ice*, edited by E. Whalley, S. J. Jones and L. W. Gold (University of Toronto Press), p. 73 ; cf. p. 80.
[51] KITAMURA, N., KASHIWASE, Y., HARADA, J., and HONJO, G., 1961, *Acta crystallogr.*, **14,** 687.
[52] HANKINS, D. B., 1970, Ph.D. Thesis, submitted in partial fulfilment of the requirements for the Ph.D., New York University.
[53] DIERCKSEN, G. H., F., and KRAEMER, W. P. (private communication).
[54] LIE, G. C., and CLEMENTI, E., 1975, *J. chem. Phys.*, **62,** 2195.
[55] DULMAGE, W. J., and LIPSCOMB, W. N., 1951, *Acta crystallogr.*, **4,** 330.
[56] AZOJI, M., and LIPSCOMB, W. N., 1954, *Acta crystallogr.*, **7,** 173.
[57] ZEISS, G. D., and MEATH, W. J., 1975, *Molec. Phys.*, **30,** 161 ; 1977, *Ibid.*, **33,** 1155.
[58] LONDON, F., 1937, *Trans. Faraday Soc.*, **33,** 8.

[59] COULSON, C. A., and EISENBERG, D. A., 1966, *Proc. R. Soc.* A, **291,** 454.
[60] PACK, G. R., WANG, H-y., REIN, R., 1972, *Chem. Phys. Lett.*, **17,** 381.
[61] REIN, R., 1973, *Adv. quant. Chem.*, **7,** 335.
[62] NG, K-C., MEATH, W. J., and ALLNATT, A. R., 1977, *Molec. Phys.*, **33,** 699.
[63] NG, K-C., MEATH, W. J., and ALLNATT, A. R., 1976, *Molec. Phys.*, **32,** 177.
[64] MULDER, F. J., and VAN HEMERT, M. (private communication).
[65] MARGOLIASH, D. J., PROCTOR, T. R., ZEISS, G. D., and MEATH, W. J., 1978, *Molec. Phys.*, **35,** 747.
[66] O'SHEA, S. F., and MEATH, W. J., 1976, *Molec. Phys.*, **31,** 515.
[67] DIERCKSEN, G. H. F., KRAEMER, W. P., and ROOS, B. O., 1975, *Theor. chim. Acta*, **36,** 249.
[68] NARTEN, A. H., and LEVY, H. A., 1969, *Science, N.Y.*, **165,** 447 ; cf. p. 449.
[69] HAJDU, F., LENGYEL, S., and PALINKAS, G., 1976, *J. appl. Crystallogr.*, **9,** 134.
[70] NARTEN, A. H., 1972, *J. chem. Phys.*, **56,** 5681.
[71] NEUMANN, D., and MOSKOWITZ, J. W., 1968, *J. chem. Phys.*, **49,** 2056.
[72] VERHOEVEN, J., and DYMANUS, A., 1970, *J. chem. Phys.*, **52,** 3222.
[73] DYKE, T. R., and MUENTER, J. S., 1973, *J. chem. Phys.*, **59,** 3125.
[74] COULSON, C. A., and EISENBERG, D., 1966, *Proc. R. Soc.* A, **291,** 445.
[75] JOHARI, G. P., and WHALLEY, E., 1976, *J. chem. Phys.*, **64,** 4484 ; (*a*) p. 4484.
[76] DANTL, G., 1962, *Z. Phys.*, **166,** 115.